12-1-1993

Neutron-Diffraction and Mössbauer-Effect Studies of $Pr_2(Fe_{1-x}Mn_x)_{14}B$

Oran Allan Pringle
Missouri University of Science and Technology, pringle@mst.edu

Jie Fu

Gary J. Long
Missouri University of Science and Technology, glong@mst.edu

William Joseph James
Missouri University of Science and Technology, wjames@mst.edu

et. al. For a complete list of authors, see http://scholarsmine.mst.edu/phys_facwork/187

Recommended Citation

O. A. Pringle et al., "Neutron-Diffraction and Mössbauer-Effect Studies of $Pr_2(Fe_{1-x}Mn_x)_{14}B$," *Journal of Applied Physics*, vol. 67, no. 9, pp. 4762-4764, American Institute of Physics Publishing LLC, Dec 1993.
The definitive version is available at https://doi.org/10.1063/1.344778

Neutron-diffraction and Mössbauer-effect studies of $Pr_2(Fe_{1-x}Mn_x)_{14}B$

O. A. Pringle and Jie Fu
Department of Physics, University of Missouri-Rolla, Rolla, Missouri 65401

Gary J. Long
Department of Chemistry, University of Missouri-Rolla, Rolla, Missouri 65401

W. J. James
Department of Chemistry and Graduate Center for Materials Research, University of Missouri-Rolla, Rolla, Missouri 65401

D. Xie and W. B. Yelon
University of Missouri Research Reactor, Columbia, Missouri 65211

F. Grandjean
Institut de Physique, Universite de Liege, B-4000 Sart Tilman, Belgium

A neutron-diffraction investigation of a series of $Pr_2(Fe_{1-x}Mn_x)_{14}B$ samples, with x values of 0.00, 0.11, 0.22, 0.30, and 0.35, reveals a preference for the manganese to occupy the $8j_2$ transition-metal site,the transition-metal site with the largest Wigner–Seitz cell volume. Similar site occupancies have been reported previously for $Er_2(Fe_{1-x}Mn_x)_{14}B$ and $Y_2(Fe_{1-x}Mn_x)_{14}B$. An analysis of the 295-K Mössbauer spectrum of $Pr_2(Fe_{0.89}Mn_{0.11})_{14}B$ indicates that the internal hyperfine fields on the six iron sites are more substantially reduced from those found in $Pr_2Fe_{14}B$ than would be expected from a simple magnetic dilution with manganese. The extent of the field reduction for a specific site increases with the number of manganese near neighbors for the site. Fits of the Mössbauer spectra of $Pr_2(Fe_{0.78}Mn_{0.22})_{14}B$, $Pr_2(Fe_{0.70}Mn_{0.30})_{14}B$, and $Pr_2(Fe_{0.65}Mn_{0.35})_{14}B$, which are paramagnetic at room temperature, give quadrupole splittings consistent with the quadrupole interactions in $Pr_2Fe_{14}B$.

The study of $R_2(Fe_{1-x}Mn_x)_{14}B$ compounds, where R is yttrium or a rare earth, provides insight into the anisotropy and magnetic exchange in the $Nd_2Fe_{14}B$-type magnets. It has been previously shown that in $Er_2(Fe_{1-x}Mn_x)_{14}B$, manganese preferentially occupies the $8j_2$ transition-metal site.[1] For $x<0.2$, the transition-metal moments align ferromagnetically in the basal plane of the tetragonal unit cell. For $x\geqslant 0.4$, the only iron magnetic moments which are ordered at 4.2 K are the $16k_1$ and $4c$ moments.[2] The manganese $8j_2$ moments order antiferromagnetically, corresponding to a strong coupling along the major disclination line, the line along which magnetic interactions are at a maximum.[3]

Manganese also preferentially occupies the $8j_2$ site in $Y_2(Fe_{1-x}Mn_x)_{14}B$.[4,5] At room temperature, all of the transition-metal magnetic moments align ferromagnetically along the c axis in both $Y_2Fe_{13}MnB$ and $Y_2Fe_{11}Mn_3B$.[5] The addition of manganese to $Y_2Fe_{14}B$ reverses the anomalous temperature dependence of the magnetic anisotropy, probably due to either a decrease in the planar contribution to the anisotropy or a change in the volume magnetostriction.[5]

In $Er_2Fe_{14}B$, the erbium is magnetic and the transition-metal moments order in the basal plane. In $Y_2Fe_{14}B$, the yttrium is nonmagnetic and the transition-metal moments align along the c axis. In contrast, in $Pr_2Fe_{14}B$, the praesodymium is magnetic and the transition-metal moments align along the c axis. Further, the addition of manganese to $Pr_2Fe_{14}B$ increases its magnetic anisotropy at 77 K.[6] The $Pr_2(Fe_{1-x}Mn_x)_{14}B$ solid solutions thus facilitate the study of the influence of different rare-earth atoms and magnetic anisotropies on the transition-metal site occupancies and magnetic moments. We report herein a neutron-diffraction and Mössbauer-effect study of $Pr_2(Fe_{1-x}Mn_x)_{14}B$.

$Pr_2(Fe_{1-x}Mn_x)_{14}B$ samples with x equal to 0.00, 0.11, 0.22, 0.30, and 0.35 were prepared using techniques described previously.[4] Small samples taken from the annealed ingots were placed in a vibrating sample magnetometer,and the Curie temperatures were determined from the magnetization-versus-temperature curves. The resulting Curie temperatures of 570, 443, 279, 154, and 95 K for the samples with x equal to 0.00, 0.11, 0.22, 0.30, and 0.35, respectively, agree well with those reported earlier for similar samples.[6]

Powder samples used for neutron diffraction and Mössbauer spectroscopy were prepared by crushing the annealed ingots to 400 mesh (0.038 mm^2) under a dry nitrogen atmosphere. The neutron-diffraction samples of about 5 g were encapsulated in a thin-walled vanadium can, and neutron-diffraction data were collected at the University of Missouri Research Reactor. The neutron wavelength used was approximately 1.3 Å, and data acquisition took about 24 h for each sample. The data were collected in four 25° intervals in 2θ from 5° to 105° and were then rebinned into 0.1° steps for analysis with a modified Rietveld code. Neutron-diffraction patterns were obtained at 623 K for $Pr_2Fe_{14}B$ and at 473 K for $Pr_2(Fe_{0.89}Mn_{0.11})_{14}B$, i.e., above their Curie temperatures. Neutron-diffraction patterns for the remaining samples were obtained at 295 K.

The neutron-diffraction refinements revealed that all of the $Pr_2(Fe_{1-x}Mn_x)_{14}B$ sample crystallized in the tetragonal $Nd_2Fe_{14}B$ structure. About 5% of α-iron was present in the samples. The 2θ diffraction regions containing the α-iron reflections were excluded from the refinements. Parameters refined included the atomic positions, the transition-metal site occupancies, lattice parameters, one overall thermal parameter, and instrumental background, zero-

 0021-8979/90/094762-03$03.00

TABLE I. Crystallographic parameters for $Pr_2(Fe_{1-x}Mn_x)_{14}B$. R_{wp} is the weighted profile R factor, and R_{exp} is the statistically expected R factor. χ^2 is R^2_{wp}/R^2_{exp}.

Parameter		x				
		0.00	0.11	0.22	0.30	0.35
Pr $4f$	x,y	0.2664(14)	0.2708(15)	0.2702(14)	0.2701(10)	0.2685(14)
Pr $4g$	x,y	0.1381(15)	0.1376(15)	0.1348(17)	0.1365(11)	0.1349(17)
TM $16k_1$	x	0.2236(15)	0.2236(7)	0.2224(7)	0.2221(6)	0.2203(9)
	y	0.5679(5)	0.5669(6)	0.5667(7)	0.5662(6)	0.5681(8)
	z	0.1269(3)	0.1279(5)	0.1287(5)	0.1294(4)	0.1311(6)
TM $16k_2$	x	0.0373(4)	0.0367(5)	0.0365(6)	0.0361(5)	0.0351(7)
	y	0.3599(4)	0.3609(6)	0.3610(7)	0.3611(5)	0.3603(7)
	z	0.1774(3)	0.1785(4)	0.1790(5)	0.1794(4)	0.1794(6)
TM $8j_1$	x,y	0.0962(5)	0.0969(7)	0.0975(7)	0.0985(6)	0.0966(10)
	z	0.2064(4)	0.2069(6)	0.2091(6)	0.2099(6)	0.2097(9)
TM $8j_2$	x,y	0.3177(5)	0.3166(10)	0.3178(19)	0.3363(48)	0.3205(117)
	z	0.2457(5)	0.2475(9)	0.2515(16)	0.2658(43)	0.2297(141)
TM $4e$	z	0.1158(7)	0.1156(9)	0.1141(9)	0.1168(7)	0.1161(10)
B $4g$	x,y	0.3722(13)	0.3697(14)	0.3669(16)	0.3670(9)	0.3720(16)
$B_{thermal}$ (Å)		0.81(4)	0.57(5)	0.34(5)	0.35(5)	0.27(8)
a (Å)		8.7754(7)	8.7840(11)	8.7726(11)	8.7937(10)	8.8027(15)
c (Å)		12.2183(15)	12.2086(19)	12.1914(20)	12.2090(17)	12.2164(26)
V (Å^3)		940.9	942.0	938.2	944.1	946.3
c/a		1.3923	1.3899	1.3897	1.3884	1.3878
R_{wp} (%)		4.48	4.37	4.12	4.08	4.10
R_{exp} (%)		1.77	1.72	1.69	1.70	1.84
χ^2		6.41	6.46	5.95	5.76	4.96
T(K)		623	463	295	295	295

point, and linewidth parameters. The refined atomic position parameters were very close to those reported previously for $Nd_2Fe_{14}B$.[7] Table I gives the crystallographic parameters for the refinements.

The neutron-diffraction analysis shows that manganese exhibits a strong preference for the $8j_2$ transition-metal site. Table II gives the refined manganese occupancies. Figure 1 is a plot of these occupancies, which are very close to those previously observed[1,4,5] in $Er_2(Fe_{1-x}Mn_x)_{14}B$ and $Y_2(Fe_{1-x}Mn_x)_{14}B$. In our refinements, the total manganese content was allowed to vary, but the transition-metal sites were constrained to be fully populated by iron, manganese, or a combination of the two. The refined manganese populations are close to the nominal compositions of x equal to 0.0, 0.1, 0.2, 0.3, and 0.4.

The manganese site occupancies are consistent with occupation of the larger-volume sites by manganese. The

TABLE II. Manganese site occupancies for $Pr_2(Fe_{1-x}Mn_x)_{14}B$. N is the number of atoms and % is the fractional occupancy.

x(refined)		$16k_1$	$16k_2$	$8j_1$	$8j_2$	$4c$	$4e$
0.111	N	1.11(21)	1.05(18)	0.78(11)	2.61(9)	0.53(7)	0.11(7)
	%	6.9	6.6	9.8	32.6	13.2	2.7
0.215	N	2.74(13)	2.40(11)	1.51(9)	4.28(8)	0.76(6)	0.36(6)
	%	17.1	15.0	18.8	53.4	19.1	9.1
0.298	n	4.15(11)	3.40(11)	2.14(7)	5.33(5)	1.07(4)	0.58(5)
	%	25.9	21.2	26.8	66.6	26.8	14.4
0.351	N	4.89(16)	3.81(16)	2.77(10)	6.03(7)	1.41(6)	0.76(7)
	%	30.5	23.8	34.6	75.3	35.4	19.0

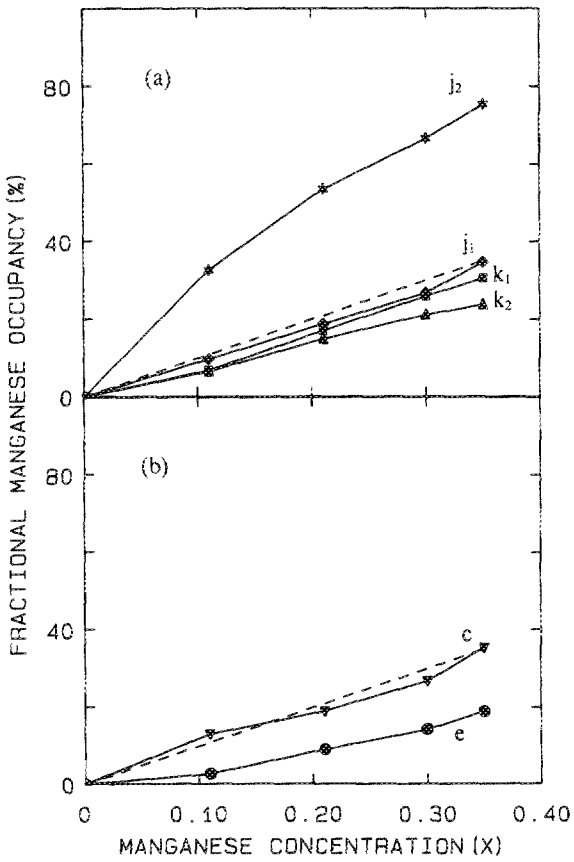

FIG. 1. The fractional manganese occupancy vs manganese concentration for $Pr_2(Fe_{1-x}Mn_x)_{14}B$. The broken line represents the value for random occupation.

TABLE III. Compositional dependence of the internal hyperfine fields in $Pr_2(Fe_{1-x}Mn_x)_{14}B$ at 295 K.

	$16k_1$	$16k_2$	$8j_1$	$8j_2$	$4c$	$4e$	$\langle H_{int}\rangle$[a]
H_{int} for $x=0.00$ (kOe)	287	306	278	342	256	279	296
H_{int} for $x=0.11$ (kOe)	177	235	132	280	115	177	195
ΔH_{int} (kOe)	110	71	146	62	131	102	101
No. of $8j_2$ NN[b]	2	2	3	0	0	2	···

[a] The area weighted average internal hyperfine field.
[b] Near neighbors.

Wigner–Seitz cell volumes[8,9] in $Pr_2Fe_{14}B$ are 11.79, 11.60, 12.16, 12.75, 12.35, and 11.87 Å^3 for the $16k_1$, $16k_2$, $8j_1$, $8j_2$, $4c$, and $4e$ sites, respectively. The $8j_2$ site has the largest volume, and the $16k_2$, $16k_1$, and $4e$ sites have the smaller volumes. Thus, in $Er_2(Fe_{1-x}Mn_x)_{14}B$, $Y_2(Fe_{1-x}Mn_x)_{14}B$, and $Pr_2(Fe_{1-x}Mn_x)_{14}B$, the manganese site occupancies are determined by void-filling constraints. Apparently, the enthalpy term outweighs the entropy term in the chemical potential in establishing the equilibrium site occupancy.

The preparation of the Mössbauer absorbers and the procedure used to fit the Mössbauer spectra have been described previously.[4,10] Mössbauer spectra were obtained at 295 and 77 K for the $Pr_2(Fe_{1-x}Mn_x)_{14}B$ samples, and at a series of temperatures for $Pr_2Fe_{14}B$. The Mössbauer-effect results for $Pr_2Fe_{14}B$ have been reported previously.[8] The $Pr_2(Fe_{0.89}Mn_{0.11})_{14}B$ spectrum has been fit with six broadened, overlapping magnetic sextets and including the site populations determined in this neutron-diffraction study. The resulting hyperfine fields for $Pr_2Fe_{14}B$ and $Pr_2(Fe_{0.89}Mn_{0.11})_{14}B$ at 295 K are given in Table III. If the hyperfine field were simply decreased by a dilution of the iron magnetic moments, the decrease in the area-weighted average internal hyperfine field would be given by $H_{int}=H_0(1-x)$, where H_0 is the field in $Pr_2Fe_{14}B$. With this model, the area-weighted average internal hyperfine field would be 263 kOe in $Pr_2(Fe_{0.89}Mn_{0.11})_{14}B$, whereas the observed value is only 195 kOe. The larger-than-expected decrease indicates an enhancement over random breakdown of the long-range iron-iron exchange coupling by the manganese. The influence of the manganese on the exchange coupling may also be observed in the changes in the internal hyperfine fields ΔH_{int} given in Table III. The $8j_1$ site, which has the largest number of $8j_2$ near neighbors,[8] and hence the most manganese near neighbors, exhibits the largest ΔH_{int} value of 146 kOe. In contrast, the $8j_2$ site, which has no $8j_2$ near neighbors, shows the smallest ΔH_{int} value of 62 kOe.

TABLE IV. Quadrupole interactions in mm/s in $Pr_2Fe_{14}B$ and quadrupole splittings in mm/s in $Pr_2(Fe_{1-x}Mn_x)_{14}B$ at 295 K.

x	$16k_1$	$16k_2$	$8j_1$	$8j_2$	$4e$	$4c$
0.00	0.296	0.292	0.281	0.667	−0.670	−0.214
0.22	0.309	0.749	0.209	1.062	0.947	0.039
0.30	0.308	0.745	0.186	1.064	0.938	0.086
0.35	0.310	0.774	0.250	1.010	0.935	0.064

The $Pr_2(Fe_{1-x}Mn_x)_{14}B$ samples with x equal to 0.22, 0.30, and 0.35 are paramagnetic at room temperature. These spectra were fit with six doublets, with relative areas that were constrained by the neutron-diffraction site populations. The quadrupole splittings for these three paramagnetic samples and the quadrupole interaction[8] for $Pr_2Fe_{14}B$ are given in Table IV. The magnitude of the quadrupole splittings for all of the paramagnetic samples are generally in agreement with the magnitude of the quadrupole interaction in $Pr_2Fe_{14}B$. The quadrupole splittings in the paramagnetic spectra need not be identical with the quadrupole interactions in the ferromagnetic spectrum, but general agreement is expected, and the magnitude of the paramagnetic splittings put an upper limit on the magnitude of the quadrupole interactions in $Pr_2Fe_{14}B$. The general consistency of the quadrupole splittings also supports the model used to fit $Y_2Fe_{14}B$,[8] $Nd_2Fe_{14}B$,[11] and $Gd_2Fe_{14}B$.[8]

The authors acknowledge support from the University of Missouri under a Weldon Spring grant.

[1] C. D. Fuerst, G. P. Meisner, F. E. Pinkerton, and W. B. Yelon, J. Less-Common Met. **133**, 255 (1987).
[2] W. B. Yelon, D. Xie, C. M. Hsueh, C. D. Fuerst, and G. P. Meisner, Phys. Rev. B **39**, 9389 (1989).
[3] R. E. Watson, L. H. Bennett, and M. Melamud, J. Appl. Phys. **63**, 3136 (1988).
[4] O. A. Pringle, G. K. Marasinghe, G. J. Long, W. J. James, W. B. Yelon, D. Xie, and F. Grandjean, J. Appl. Phys. **64**, 5580 (1988).
[5] O. Moze, L. Pareti, M. Solzi, F. Bolzoni, W. I. F. David, W. T. A. Harrison, and A. W. Hewat, J. Less-Common Met. **136**, 375 (1988).
[6] M. Q. Huang, E. B. Boltich, and W. E. Wallace, J. Less-Common Met. **124**, 55 (1986).
[7] J. F. Herbst, J. J. Croat, F. E. Pinkerton, and W. B. Yelon, Phys. Rev. B **29**, 4176 (1984).
[8] F. Grandjean, G. J. Long, O. A. Pringle, and J. Fu, Hyp. Int. (in press).
[9] L. Gelato, J. Appl. Crystallogr. **14**, 141 (1981).
[10] Y. C. Yang, D. E. Tharp, G. J. Long, O. A. Pringle, and W. J. James, J. Appl. Phys. **61**, 4343 (1987).
[11] F. Grandjean, G. J. Long, D. E. Tharp, O. A. Pringle, and W. J. James, J. Phys. (Paris) Colloq. **49**, C8-581 (1988).